ASTRONOMY & ASTROPHYSICS
SUPPLEMENT SERIES

Astron. Astrophys. Suppl. Ser. **137**, 385–389 (1999)

Effect of anisotropic imaging in off-axis adaptive astronomical systems

V.V. Voitsekhovich[1] **and S. Bara**[2]

[1] Instituto de Astronomia, UNAM AP 70-264 Cd. Universitaria, 04510 Mexico D.F., Mexico
e-mail: voisteko@astroscu.unam.mx
[2] Area de Optica, Departamento de Fisica Aplicada, Facultade de Fisica, Universidade de Santiago de Compostela, Campus Sur, 15706 Santiago de Compostela, Galicia, Spain
e-mail: fagosxbv@usc.es

Received October 7, 1998; accepted March 23, 1999

Abstract. Effect of anisotropic imaging arising due to the off-axis adaptive correction is considered. The main manifestation of this effect is that the isophotes of the image of a star separated by some angular distance from the guide one have a non-circular form. It is shown that the effect of interest depends strongly on the observation conditions, and under certain conditions the image width in direction towards the guide star can be up to two times wider than in the transversal one. The results obtained can be used in practice for the reconstruction or calibration of images obtained after the off-axis adaptive correction.

Key words: atmosphere effects — instrumentation: adaptative optics

1. Introduction

The performances of off-axis adaptive correction are of interest for astronomical observations because such an approach allows to avoid certain difficulties dealing with observations of weak stars. The approach itself assumes that some bright enough guide star (a natural or an artificial one) is chosen to perform the measurement of atmospherically distorted wavefronts, then the data obtained are applied for an adaptive correction. This method allows one to improve the images of stars located in some area around the guide star. However unlike the usual on-axis adaptive correction, the off-axis one produces some specific distortions on the corrected image.

To predict main effects arising in off-axis adaptive correction, it is sufficient to consider two stars (say, the guide and the observed one) separated by some angular distance. For this case the quality of off-axis correction is determined by the residual structure function $D_{\rm R}$ which shows the degree of correlation between the wavefronts produced by the stars at the aperture of the telescope. It has been shown (Fried 1982; Vitrichenko et al. 1984; Chassat 1989) that, even for the perfect adaptive correction, the residual structure function is an anisotropic one because the light from the stars passes through different paths in the atmosphere. As a consequence of this phenomena, the long-exposure point spread function (PSF) of the observed star will be anisotropic, i.e. the isophotes of the observed image will have a non-circular form.

The effect of interest has recently been found experimentally (Close 1998). The authors noticed that "Off-axis guide stars produce an elongation in the science object's PSF towards the direction of the guide star" and pointed out that the anisoplanatic phenomena is responsible for this effect. In this paper we present a detailed theoretical treatment of this effect for the case of perfect off-axis adaptive correction considering how the anisotropy of corrected image depends on the observation conditions, angular separation between the stars and telescope size. The results obtained can serve for the reconstruction or calibration of wide-field images provided by systems with adaptive correction.

2. Long-exposure PSF in off-axis adaptive system

Let S_1 and S_2 be the turbulence-induced phase fluctuations at the aperture associated with the observed and the guide star, respectively. In the case of perfect adaptive correction the residual phase fluctuation $S_{\rm R}$ associated with the observed star is $S_{\rm R} = S_1 - S_2$. Since in the astronomical observations the turbulence-induced amplitude fluctuations are practically negligible (Roddier 1981), the long-exposure PSF P of the observed star can be

Send offprint requests to: V.V. Voitsekhovich

written as:

$$P(\boldsymbol{r}) = \left(\frac{kA}{2\pi f}\right)^2 \int_G \mathrm{d}^2\rho_1 \int_G \mathrm{d}^2\rho_2 \exp\left\{-\frac{1}{2}D_\mathrm{R}(\boldsymbol{\rho}_1,\boldsymbol{\rho}_2)\right\} \times \cos\left\{\frac{k}{f}\boldsymbol{r}\cdot(\boldsymbol{\rho}_1-\boldsymbol{\rho}_2)\right\}, \tag{1}$$

where $\boldsymbol{r}$ denotes the two-dimensional vector in the focal plane, k is the wavenumber, f is the focal length of the telescope, G denotes that the integration is performed over the telescope aperture, and

$$D_\mathrm{R}(\boldsymbol{\rho}_1,\boldsymbol{\rho}_2) = \left\langle [S_1(\boldsymbol{\rho}_1) - S_2(\boldsymbol{\rho}_2)]^2 \right\rangle$$

is the residual structure function of phase. Because we are interested to consider only the properties of the turbulence-induced PSF, it is assumed in derivation of Eq. (1) that the telescope itself has diffraction-limited image quality.

To calculate D_R, let us introduce the three-dimensional Cartesian coordinate system in such a way that the observed star is on the Z-axis, the propagation vector $\boldsymbol{n}$ of the initially plane wave produced by the guide star at the upper boundary of the atmosphere lies in the XZ plane, and XY plane is the aperture plane. Under these conditions and for the case of Kolmogorov turbulence, D_R can be expressed as (Voitsekhovich et al. 1998):

$$D_\mathrm{R}(\boldsymbol{\rho}=\boldsymbol{\rho}_1-\boldsymbol{\rho}_2) = 5.83k^2 \int_0^L \mathrm{d}z C_n^2(z) \times \left[\rho^{5/3} + (n_\perp z)^{5/3} - \frac{1}{2}|\boldsymbol{\rho}+\boldsymbol{n}_\perp z|^{5/3} - \frac{1}{2}|\boldsymbol{\rho}-\boldsymbol{n}_\perp z|^{5/3}\right], \tag{2}$$

where L is the propagation distance, C_n^2 denotes the refractive index structure characteristic, ρ and $n_\perp$ stand for the modulus of the corresponding vectors, and $\boldsymbol{n}_\perp$ is the projection of the propagation vector $\boldsymbol{n}$ on the aperture plane. For the small angular star separations γ which are of interest in astronomical applications, the vector $\boldsymbol{n}_\perp$ can be expressed as

$$\boldsymbol{n}_\perp \approx (\gamma, 0),$$

where γ is given in radians.

As one can see from Eq. (2), the residual structure function is an anisotropic but still a homogeneous function of the vector $\boldsymbol{\rho}$. For any fixed $\boldsymbol{n}_\perp$ (or, in other words, for any fixed separations γ between the stars), it can be considered in polar coordinates as a function of two arguments: the module ρ and the polar angle φ of the vector $\boldsymbol{\rho}$:

$$D_\mathrm{R}(\rho,\varphi) = 5.83k^2 \int_0^L \mathrm{d}z C_n^2(z) \times \left[\rho^{5/3} + (\gamma z)^{5/3} - \frac{1}{2}r_+^{5/3} - \frac{1}{2}r_-^{5/3}\right], \tag{3}$$

where $r_\pm = \sqrt{\rho^2 + \gamma^2 z^2 \pm 2\rho\gamma z\cos\varphi}$.

Taking into account the homogeneity of D_R and applying an approach similar to that used in Tatarski (1968) for the integration of four-dimensional isotropic functions, we can reduce the four-times integral (1) to the two-times one as:

$$P(\boldsymbol{r}) = \left(\frac{kA}{2\pi f}\right)^2 \frac{D^2}{2} \times \int_0^D \mathrm{d}\rho\rho \left[\arccos\left(\frac{\rho}{D}\right) - \frac{\rho}{D}\sqrt{1-\frac{\rho^2}{D^2}}\right] \times \int_0^{2\pi} \mathrm{d}\varphi \exp\left\{-\frac{1}{2}D_\mathrm{R}(\rho,\varphi)\right\} \cos\left[\frac{k}{f}r\rho\cos(\varphi-\theta)\right], \tag{4}$$

where D is the telescope diameter, and r and θ are the modulus and the polar angle of the vector $\boldsymbol{r}$, respectively.

Equation (4) allows for a direct interpretation in the framework of linear incoherent imaging systems. The PSF P is the Fourier transform of the overall optical transfer function (OTF) which is the product of the diffraction limited telescope OTF H_T

$$H_\mathrm{T}(\rho) = \left(\frac{2}{\pi}\right)\mathrm{circ}\left(\frac{\rho}{D}\right)\left[\arccos\left(\frac{\rho}{D}\right) - \frac{\rho}{D}\sqrt{1-\frac{\rho^2}{D^2}}\right]$$

and the residual atmospheric OTF H_C

$$H_\mathrm{C}(\rho,\varphi) = \exp\left\{-\frac{1}{2}D_\mathrm{R}(\rho,\varphi)\right\}.$$

Applying to Eq. (4) the convolution theorem, the long-exposure PSF can be described as the bidimensional convolution of the telescope diffraction-limited PSF (Fourier transform of H_T) with the Fourier transform of H_C. Note that while the telescope diffraction-limited PSF is rotationally symmetric and has a fixed size, the Fourier transform of H_C will in turn show a variable size and a variable degree of anisotropy, depending on γ and on the profile $C_n^2(z)$ of refractive-index structure characteristic.

In general grounds, for big enough values of γ, the size and shape of the long-exposure PSF will be determined by the residual uncorrected atmospheric turbulence, since in those cases H_C has a noticeably smaller width in the frequency space than H_T. In particular, for very big γ the long-exposure PSF is expected to be wide and nearly symmetrical due to the progressive decorrelation between S_1 and S_2. On the other hand, in the region of small γ, the long-exposure PSF also becomes nearly symmetrical since the off-axis perfect correction is efficient enough as to nearly compensate the phase distortions affecting S_1. In this zone the resulting long-exposure PSF size and shape are determined mainly by the diffraction-limited telescope PSF. Between those two regions, a point of maximum anisotropy of the long-exposure PSF is expected to be found.

From the physical point of view the effect of anisotropic imaging arises because there is no rotational symmetry in the system formed by the guide and the observed stars. This lack of rotational symmetry results in anisotropic cross-correlations between the phase fluctuations produced by both stars. Since the quality of off-axis correction is determined by the degree of cross-correlations, this quality will also depend on the direction. The size of the corrected image will be different in different directions, giving rise to the anisotropic effect.

3. Calculation results

As it follows from (2, 3), one needs to apply some model of C_n^2 profile in order to calculate the PSF of interest. A convenient C_n^2 profile corresponding to the night-time observation conditions was suggested by Hufnagel (1974). This model is an analytical approximation of the experimental data, and in r_0 parametrization (r_0 is the Fried parameter), this profile is expressed as (Kouznetsov et al. 1997):

$$C_n^2(z) = C_0 r_0^{-5/3} k^{-2} \times \left[\left(\frac{z}{z_0} \right)^{10} \exp\left\{ -\frac{z}{z_1} \right\} + \exp\left\{ -\frac{z}{z_2} \right\} \right], \qquad (5)$$

where $C_0 = 1.027\ 10^{-3}$ m^{-1}, $z_0 = 4.632\ 10^3$ m, $z_1 = 10^3$ m, $z_2 = 1.5\ 10^3$ m.

The calculation results with Eqs. (3-5) are presented in Figs. 1-4.

Figure 1 presents some examples of PSF's calculated for different star separations. The graphs at the left-side show the images while the corresponding isophotes of PSF are presented in the right-side graphs. One can see that the isophotes have a non-circular form that indicates clearly an anisotropy in PSF. Note that the PSF's are wider in the guide star direction (horizontal direction) than in the transversal one (vertical direction).

In what follows we characterize the degree of anisotropy of PSF by its elongation towards the direction of the guide star. This elongation is calculated as the ratio of PSF's maximum width to the minimum one at the 0.5 level of PSF.

Figures 2-4 shows the elongation versus the star separation, Fried parameter and telescope diameter, respectively.

We show in the graphs above the elongation as a function of the Fried parameter r_0. However if one is interested in wavelength dependence, it can be calculated using the following formula

$$r_0 = 0.185 \lambda^{6/5} \left[\int_0^L \mathrm{d}z C_n^2(z) \right]^{-3/5},$$

where λ denotes the wavelength.

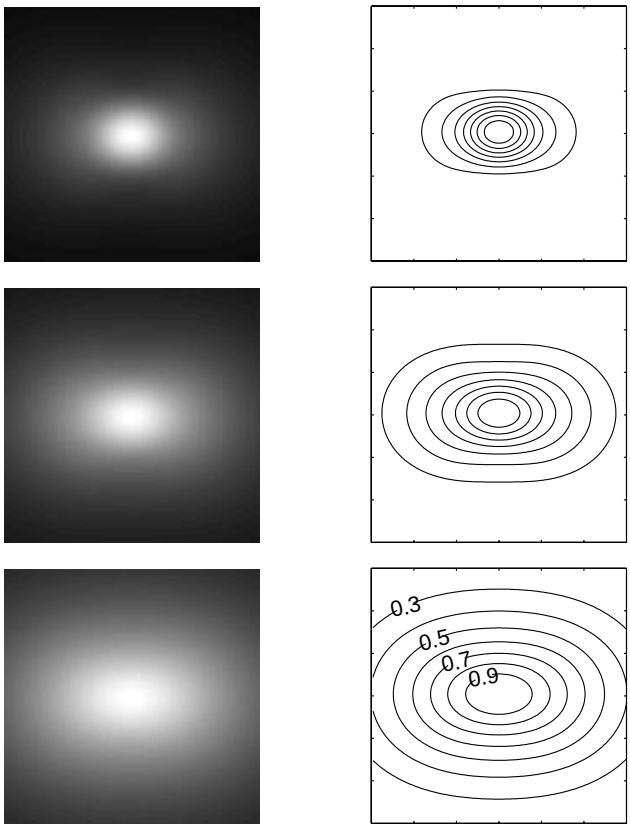

Fig. 1. Examples of anisotropic PSF's. The PSF's are elongated towards to the direction of the guide star. The PSF's have been calculated for the following conditions: the Fried parameter $r_0 = 0.2$ m, the telescope diameter $D = 2$ m, the star separations $\gamma = 6$, 7.7 and 10 arcsec (from the top to the bottom)

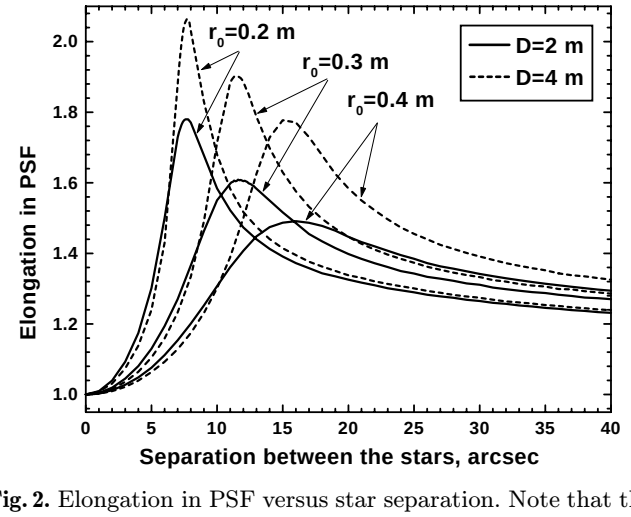

Fig. 2. Elongation in PSF versus star separation. Note that the elongation decreases with the increase of Fried parameter. In other words, the longer is the wavelength, the smaller is the elongation

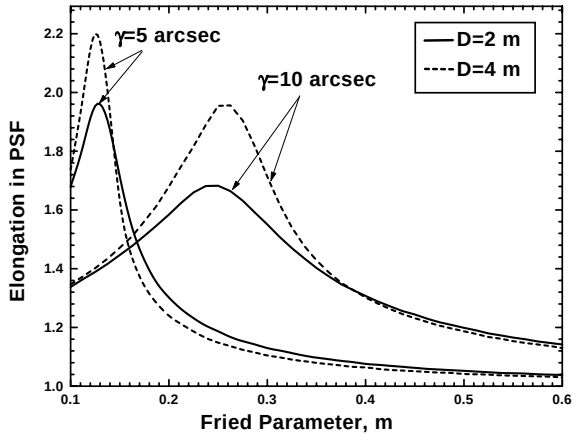

Fig. 3. Elongation in PSF versus Fried parameter

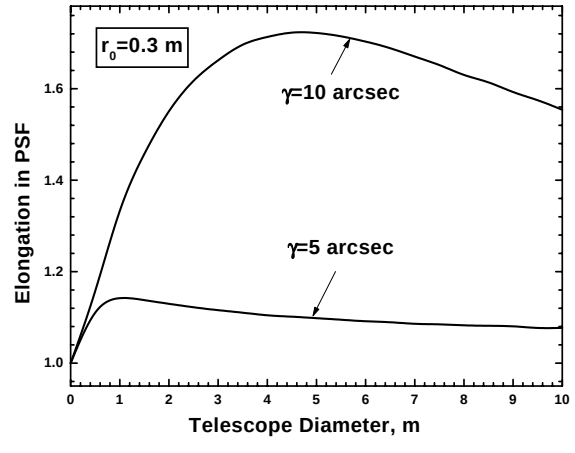

Fig. 4. Elongation in PSF versus telescope diameter

It was recently reported by Close (1998) that "Off-axis guide stars produce an elongation in the science object's PSF towards the direction of the guide star (usually about $0.15''$ of elongation at $12''$ radial distances in J band at CFHT)". Unfortunately, the information provided in this paper is not sufficient to perform a direct quantitative comparison with our theoretical results. Among other factors, the length difference between the major and minor axes of the observed star depends on the PSF level where the PSF size is measured, and this information is not available in the quoted work. We can, nevertheless, give some data about the expected axes length difference as computed from Eq. (4). Let us consider the case of a 4-m class telescope working at the J-band (1.25 microns) with $r_0 = 0.4$ m, C_n^2 profile specified by Eq. (5) and a separation $\gamma = 12''$ between the guide and observed stars. With the assumed parameters, the major and minor axes of the observed star image (measured at the PSF normalized isophote 0.25) will be $0.27''$ and $0.14''$, respectively, showing an excess length of $0.13''$ towards the direction of the guide star. This excess length will depend on the PSF level chosen to measure it, as it has been already mentioned, and in this example it ranges from $0.04''$ at PSF level 0.5 to $0.20''$ at PSF level 0.1.

4. Conclusions

The theoretical analysis presented in the paper has shown that the off-axis adaptive optics correction produces the elongation in the science objects' PSFs. This elongation is directed towards the guide star and has a variable magnitude depending on the angular separation between the science object and the guide star, the telescope diameter, the Fried parameter and the Cn2 profile. This elongation effect has recently been found in the experimental observations made with the AO system at the CFHT in Mauna Kea (Close 1998).

In order to concentrate on the essential features of the anisotropic imaging, two main simplifications have been made through this paper.

First, we have considered the case of adaptive system with the perfect correction. This assumption has permitted us to stress out the physics of anisotropic imaging leaving aside engineering details related to the partial correction. However, in real off-axis AO systems the residual distortion arising due to the partial correction is an additional source of degradation of the PSF which contributes to its widening but keeps it symmetric. This widening obscures partially the effect of elongation, especially for those systems with the low-order AO correction. The rapid developing of AO technology, however, makes us expect that the AO systems will approach the perfect ones that is the case considered here.

Second, the calculations have been made making use of the conventional Kolmogorov model that assumes an infinite outer scale of the turbulence. In reality, the outer scale is finite, with a magnitude dependent on the observation place and atmospheric conditions, and it may vary from several meters to several hundred meters. According to our preliminary estimations, the finite outer scale affects mainly the asymptotic behavior of the elongation, and its influence is pronounced when the outer scale magnitude is small. As an example let us consider how this effect will change the graphs in Fig. 1. For the Kolmogorov model the elongation tends asymptotically to the unity, but at a very slow rate. However, if the outer scale effect is taken into account, the graphs will approach the unity faster. From the experimental point of view it means that the smaller is the outer scale, the quicker the elongation will disappear with the increase of star separations.

A quantitative comparison of theoretical predictions with the real observation data is also of interest. In order to perform such a comparison, the simplified model used in the paper can be easily extended for the case of partial correction AO correction and finite outer scale, once the additional information is available. Along with the

observation data, this information has to include the parameters of the AO system, the Cn2 profile, and, maybe, the outer scale magnitude which have to be measured during the observations. Such measurements can be performed in a quasi-real time applying for example G-SCIDAR (Avila et al. 1997).

Acknowledgements. This work was supported by Ministerio de Educacion y Cultura, Spain, Ref.: SAB1995-0729 and by Sistema Nacional de Investigadores, Mexico.

References

Avila R., Vernin J., Masciadri E., 1997, Appl. Opt. 36, 7898
Chassat F., 1989, J. Optics (Paris) 20, 13
Close L.M., Roddier F.J., Roddier C.A., Graves J.E., Northcott M.J., Potter D., 1998, Proc. SPIE 3353, 406
Fried D.L., 1982, J. Opt. Soc. Am. 72, 52
Hufnagel R.E., 1974, in Optical Propagation through Turbulence, OSA Technical Digest Series. OSA, Washington, D.C., 1974, p. WA1
Kouznetsov D., Voitsekhovich V.V., Ortega-Martinez R., 1997, Appl. Opt. 36, 469
Roddier F., 1981, in Progr. Opt. 19, 283
Tatarski V.I., 1968, The Effects of the Turbulent Atmosphere on Wave Propagation, National Science Foundation Report TT-68-50464
Vitrichenko E.A., Voitsekhovich V.V., Mishchenko M.I., 1984, News of Academy of Sciences USSR: Atmospheric and Oceanic Physics 20, 870
Voitsekhovich V.V., Orlov V.G., Cuevas S., Avila R., 1998, A&AS 133, 427